ILASS–Europe 2017, 28th Conference on Liquid Atomization and Spray Systems, 6-8 September 2017, Valencia, Spain
http://dx.doi.org/10.4995/ILASS2017.2017.5051

Binary cavitation in a transparent three hole GDI nozzle

Humberto Chaves *[1], Sebastian Donath [1]
[1]Institute for Mechanics and Fluiddynamics, Technical University of Freiberg, Germany
*Corresponding author: Humberto.Chaves@imfd.tu-freiberg.de

Abstract
A more or less real size three hole (0.1 mm diameter) transparent injection nozzle was made with 120° between the orifices and an inclination of 20° to the injector axis. The geometry is similar to that of a multi hole GDI injector. Experiments are performed using n-pentane and α-methyl-naphtalene mixtures in varying composition. The flow in the orifices is observed under submerged injection conditions from downstream looking in direction of the injector using a beam splitter plate for illumination with the light from a Minilite NdYag laser that was made incoherent by fluorescence in a cuvette filled with a dilute rhodamine-ethanol mixture. The images show the appearance of cavitation depending on the cavitation number as well as on the composition of the mixture. The behaviour is not what can be expected from equilibrium thermodynamics. Due to the transient nature of the flow the n-pentane concentration cannot attain the equilibrium value one would expect and cavitation occurs at higher cavitation values. Diffusion appears to play a role in the onset appearance of cavitation for binary mixtures.

Keywords
Binary cavitation, real size transparent nozzle, fuel injection.

Introduction
The internal flow of gasoline direct injection nozzles has been investigated in the last years intensively. X-ray phase contrast imaging [1] allows visualizing the density gradients in the nozzle orifices of aluminium nozzles using very short high energy x-ray pulses from the APS Electron Storage Ring, Argonne National Laboratory. These images have shown that the flow can show hydraulic flip and cavitation in real size geometries. These results corroborate the results obtained in large scaled up transparent acrylic models of GDI multi-hole injectors, [2]. Characteristic for multi-hole injectors is the small length to diameter ratio of the orifices. The counter bore with a larger diameter does not have a direct contact with the fluid, [1] and is therefore mainly important for reducing the L/D ratio. Already in the early work with cavitating nozzles Lichtarowicz [3] noted “The function of the orifice bore, which must be at least one diameter long, is to stabilize the cavitation bubble. If the bore length is insufficient and the orifice tends to be a plate orifice cavitation occurs in bursts.” This result is found in new results for GDI nozzles [4] that show flapping in timescales “in the order of a hundredth of a millisecond “. In the case of longer orifices the length of the cavitation zone in the orifice also fluctuates [5] with frequencies of about 29 kHz. Therefore, when taking instantaneous images of cavitation there will be large scatter of the cavitation length within the nozzle. There have been some real size transparent nozzles for Diesel injector geometries, e.g. [6-8]. However, the geometry of multi-hole GDI injectors is more complex and what is more demanding is that gasoline is an aggressive medium for acrylics. This is more so when ethanol is contained in the fuel. Therefore, transparent nozzles for gasoline fuels have to be made of glass. To date no real size transparent nozzle for GDI multi-hole injectors is known to the authors. This is why measurable spray and nozzle properties are compared with the results of CFD simulations, e.g. [9,10]. Glass is a material that imposes limitations to the length to diameter ratio that can be achieved. Due to the brittleness of glass very short nozzles would require some kind of support as was done by [6] for acrylic nozzles for diesel injection. In the present paper a first step to develop a nozzle type and methodology that allows to study real size GDI nozzle flow. The length of the orifices in the present case is not yet realistic.

Gasoline fuels are never pure liquids except for a few comparison tests. They are composed of many different components that have a large range of fuel properties. The most important one for cavitation in the orifices of injectors is the vapour pressure. In the case of a mixture of pure liquids an equilibrium boiling line can be derived using thermodynamics. In mixture thermodynamics the concentration of each component is calculated for each phase. Except for azeotropic mixtures it does not have the same value in each phase. This is the basis for distillation. However, the flow in the orifices of injection nozzles is a very transient process and there is no time for establishing equilibrium. This is the basic question behind this work.

This work is licensed under a Creative Commons 4.0 International License (CC BY-NC-ND 4.0).
EDITORIAL UNIVERSITAT POLITÈCNICA DE VALÈNCIA

Material and methods

The core of the work presented here is the development of a transparent multi-hole real size nozzle similar to a gasoline direct injection (GDI) nozzle. There have been various concepts for transparent nozzles [e.g. 11,12], they have in common that they use acrylics as a nozzle material. This material can be used when looking into diesel injection nozzles, however is has the drawback that when using ethanol as a fuel, the nozzle will only survive a couple of injections. Many of the modern gasoline blends contain ethanol and other components that will sooner or later damage the nozzle. Therefore, glass was chosen as a material for the nozzle. Glass is a material that requires a completely different handling than acrylics. Most of the work was performed on a diamond wire saw controlled with a microscope coupled to a CCD camera.

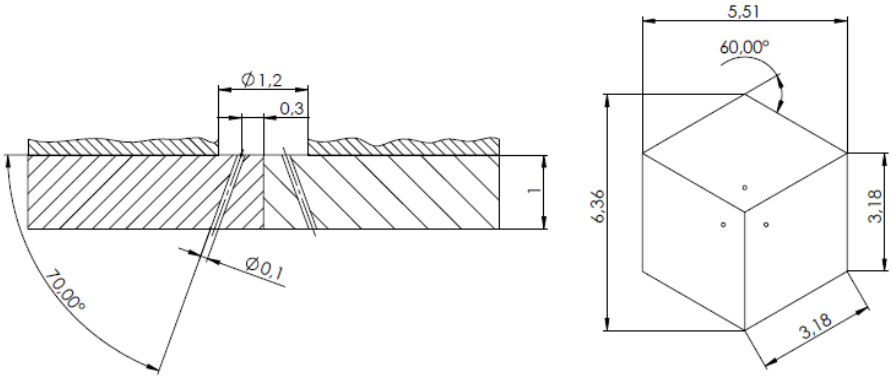

Figure 1. side view and top view of the glass nozzle. It is composed of three rhombic slides of glass each with one orifice.

Once the three rhombic slides, Figure 1 had been cut they were polished and then glued onto a diesel injector which had been ground down to the tip of the needle as can be seen on Figure 2. The first crucial part of this procedure is the positioning of the three rhombi relative to shortened sac hole of the injector, which is performed under a binocular microscope. The second difficulty was placing minute amounts of epoxy glue between the rhombi using a needle tip to seal the contact lines between them. Capillary forces let the glue flow into the thin crevice between the rhombi and form a smooth surface. Once the right position and amount of glue had been achieved the whole injector was put in an oven for curing the epoxy glue, after many trials.

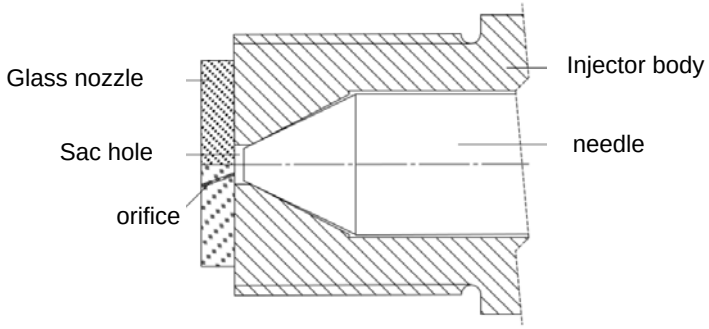

Figure 2. side view of the tip of the injector with the glass nozzle each with one orifice.

Figure 3 shows the experimental set-up. The injector tip is inserted into the injection chamber and pressed to seal the system. The fuel is filled by gravity into the not yet pressurized reservoir, then the appropriate valves are closed and the reservoir is pressurized using nitrogen from a bottle. A Bourdon pressure gauge is used to preset the injection pressure. Both the pressure histories of injection and back pressure are measured using Kistler absolute pressure sensors attached to the corresponding bridge amplifiers. Both these signals as well as the trigger signals for the Nd-YAG pulse laser are recorded simultaneously on a LeCroy digital oscilloscope, not shown here. This allows measuring the exact pressure levels present at every instant of image acquisition. The images are recorded at 14 images per second. The camera delivers the appropriate trigger signals and is started with the same signal that opens the magnetic valve that starts the injection. The back pressure can be preset using compressed air but usually it starts at atmospheric pressure and due to the displacement of air in the injection chamber by the injected fuel the air contained in the compression vessel is compressed. This leads to a slow variation of back pressure whilst the injection pressure remains constant. Every new run will give a series of images for an increasing back pressure and therefore cavitation number.

This work is licensed under a Creative Commons 4.0 International License (CC BY-NC-ND 4.0).

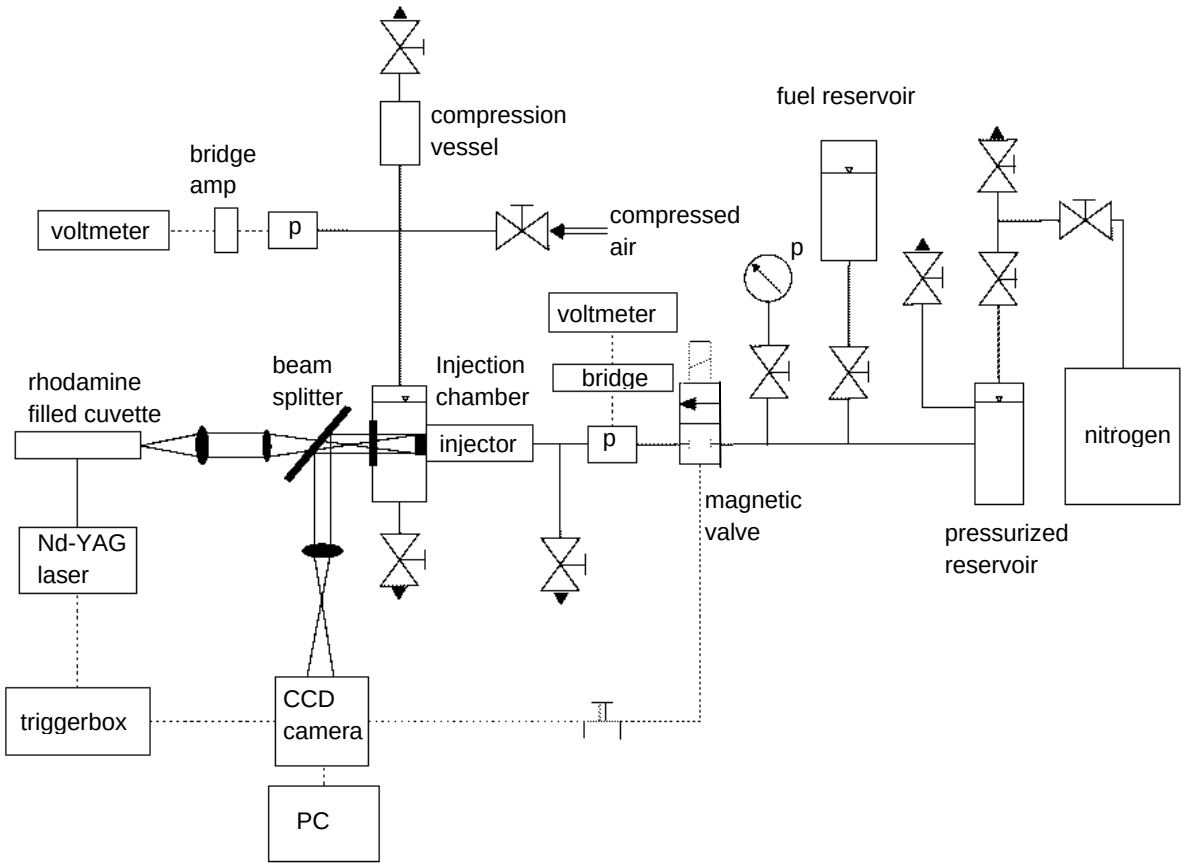

Figure 3. Schematic diagram of the experimental set-up.

The optical set-up results from the nozzle geometry and the limited depth of field of microscopic imaging. It is not possible to image all the orifices with an acceptable resolution when looking from the side as has been previously done for single orifices or for orifices that are aligned in one plane, see e.g. [13]. Here, a different approach was chosen. Both the top surface of the injector on which the nozzle is glued as well as the tip of the injector needle has been polished. This allows illuminating from the downstream side. Simultaneous observation is achieved with a beam splitter plate positioned behind the injection chamber window opposite to the injector tip. Figure 4 shows four images taken with no flow but a different fuel filling of the injection chamber. The volume fraction φ_2 of n-pentane in the mixture with α-methyl-naphtalene has been varied. The resulting difference of refractive index relative to the refractive index of the glass of the nozzle is shown above each image.

On Figure 4 various observations can be made. First one sees the polished but scratched metallic surface of the tip of the injector body and the needle tip. We decided to leave the scratches since they allow a simple focusing on the plane of the orifice inlets. The second obvious features are the glue joints between the rhombi that compose the nozzle. They appear dark due to the strong refractive index mismatch relative to the glass. The inner dark circle is the shadow of the sac hole on the needle. One can also see that the needle is at different rotation angles using e.g. the scratches or a dark feature at the rim. However, the most important features are the nozzle orifices. They can be clearly seen on image a). There are to be some dark shadows on the image of the orifices in this case. The refractive index mismatch between the glass and the fluid causes reflections and refractions at the interface leading to these intensity modulations. With decreasing volume fraction of n-pentane in the mixture the refractive index increases. In the case of image c) there is a match between the fluid and the glass. The orifices seem to disappear. In the case d) where the index of the fluid is higher than that of the glass the spurious reflections disappear. It requires some practice and comparison with these images with no flow to distinguish the reflections from cavitation voids. One can also observe that the orifice inlets are sharply imaged whereas the outlets are out of focus. This is due to the limited depth of field of the microscope objective that was used, about 0.3 mm. It is a compromise between depth of field, optical resolution, optical sensitivity and working distance. It has a working distance of 50 mm, which may appear large but keep in mind that a beam splitter plate and the injection chamber with its window are installed between the nozzle and the front lens of the objective. Its aperture gives both a good resolution and a moderate depth of field. However, even with a fully open aperture and the

This work is licensed under a Creative Commons 4.0 International License (CC BY-NC-ND 4.0).

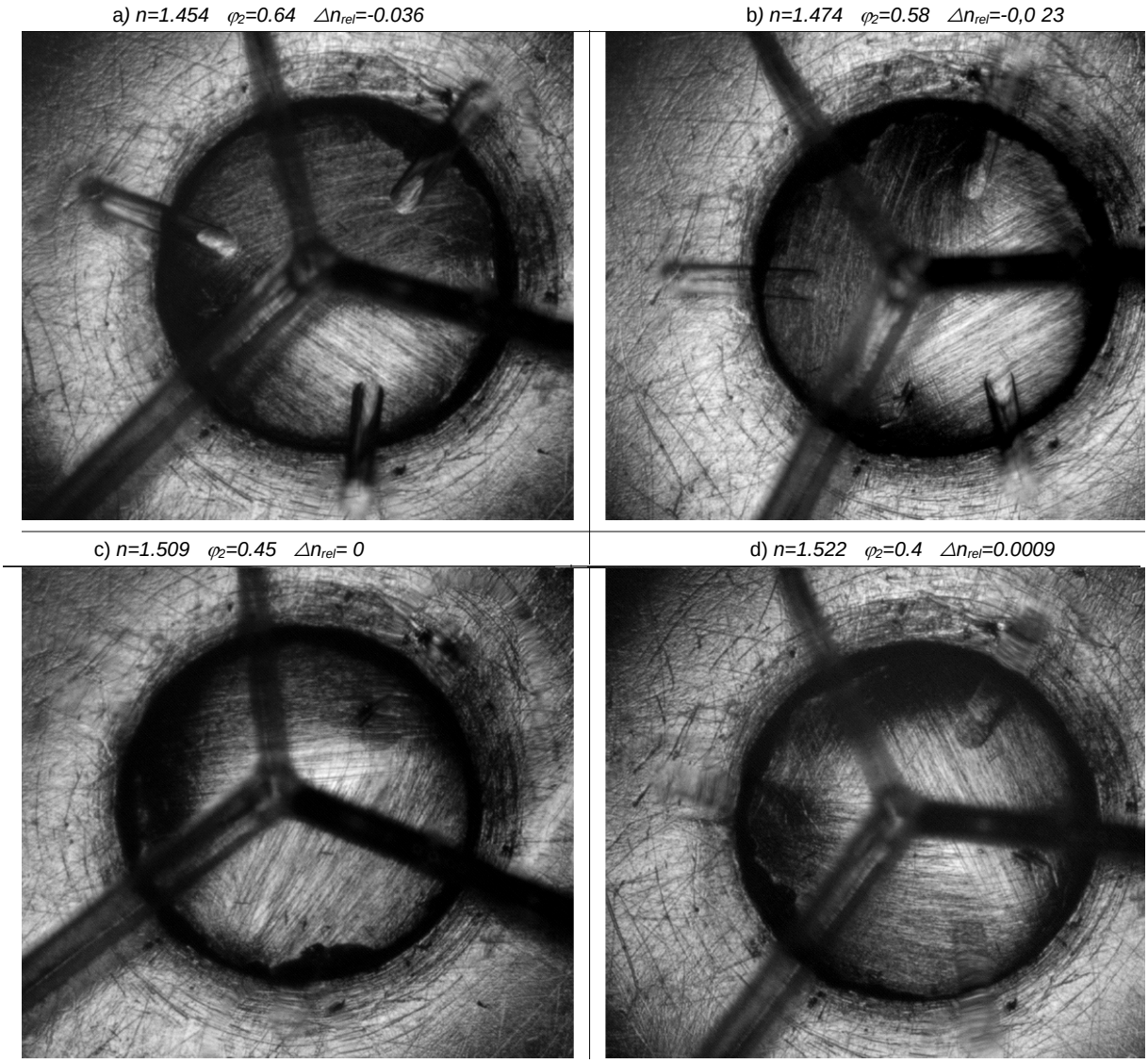

Figure 4. Optical image quality depending on the volume fraction φ_2 of n-pentane in the mixture with α-methyl-naphtalene, the dark circle in the middle is the shadow of the sac hole of 1.2 mm in diameter

sensitivity is relatively low also due to the illumination from the view direction. This is the reason for the use of a more energetic pulsed light source. For back lit images LEDs or a Nanolite flash lamp are sufficient, see [e.g. 13,14]. Here, a frequency doubled Nd-YAG laser, MiniLite is used. To get rid of the coherence the laser light it is pointed at a small cuvette with a dilute solution of Rhodamine in ethanol. The fluorescence light from the fluorophore is collected with lenses at right angle to the incidence direction of the laser light and focused onto a plastic optical fibre, not shown on Figure 3. The other end of the fibre is the incoherent pulsed light source with 5ns pulse width and sufficient energy to modulate the images. Due to the fluorescence the peak intensity is at wavelength of 590 nm vs. 532 nm of the laser.

Table 1 shows a list of the properties of the binary mixtures used for the experiments. Also two vapour pressure values are included; one based on an ideal mixture and one using a molecular simulation model (COSMOThermX). The later value is used to calculate the cavitation number for each image acquired since little data is available on this binary mixture. Here the definition of the cavitation number introduced by Bergwerk [15] is used:

$$Ca = (p_{inj}-p_{ch})/(p_{ch}-p_{vm}). \quad (1)$$

This work is licensed under a Creative Commons 4.0 International License (CC BY-NC-ND 4.0).

Table 1. List of the binary mixtures of n-pentane with α-methyl-naphtalene used for the experiments .

Refractive index measured: n	Volume fraction n-pentane: φ_2	Vapor pressure: p_{vi} Ideal mixture [hPa]	Vapor pressure: p_{vm} Molecular simulation [hPa]
1.454	0.65	386.2	431.1
1.474	0.58	354.1	409.8
1.509	0.45	281.9	357.8
1.522	0.4	253.1	334.4

Results and discussion

Every experiment is initiated by opening of the magnetic valve. It last for 2 to 3 seconds giving a sequence of 30 to 40 images with increasing cavitation number. Once the image and oscilloscope data have been stored a next run can be initiated provided there is still enough fuel in the pressurized reservoir. Due to the way the nozzle has been produced and to the wish of having complete sets of data for all mixtures before the nozzle breaks the maximum injection pressure used up to now has been limited to ca. 1.5 MPa. This is however sufficient to cover a range of cavitation numbers which are characteristic for the onset and extent of cavitation to the orifice exit. At much higher cavitation numbers there a few visible differences in the nozzle flow; cavitation always reaches up to the exit of of the orifice, i.e. supercavitation. Figure 5 shows exemplarily four images taken from one run with increasing chamber pressure, constant injection pressure and thus a variation of the cavitation number. One can see that the cavitation behaviour is different for all three orifices. This is due to the differences of the inlet corner of each orifice. Glass has the disadvantage that it can chip and standard microscope images with a large magnification have shown that the left orifice inlet is chipped. This disturbance promotes cavitation. The right orifice is also slightly chipped whereas the middle one has a smooth edge. It is not oriented to the injector axis. The other orifices also show a deviation from symmetry. The nozzle is “handmade”. This is occurs however also in series injectors.

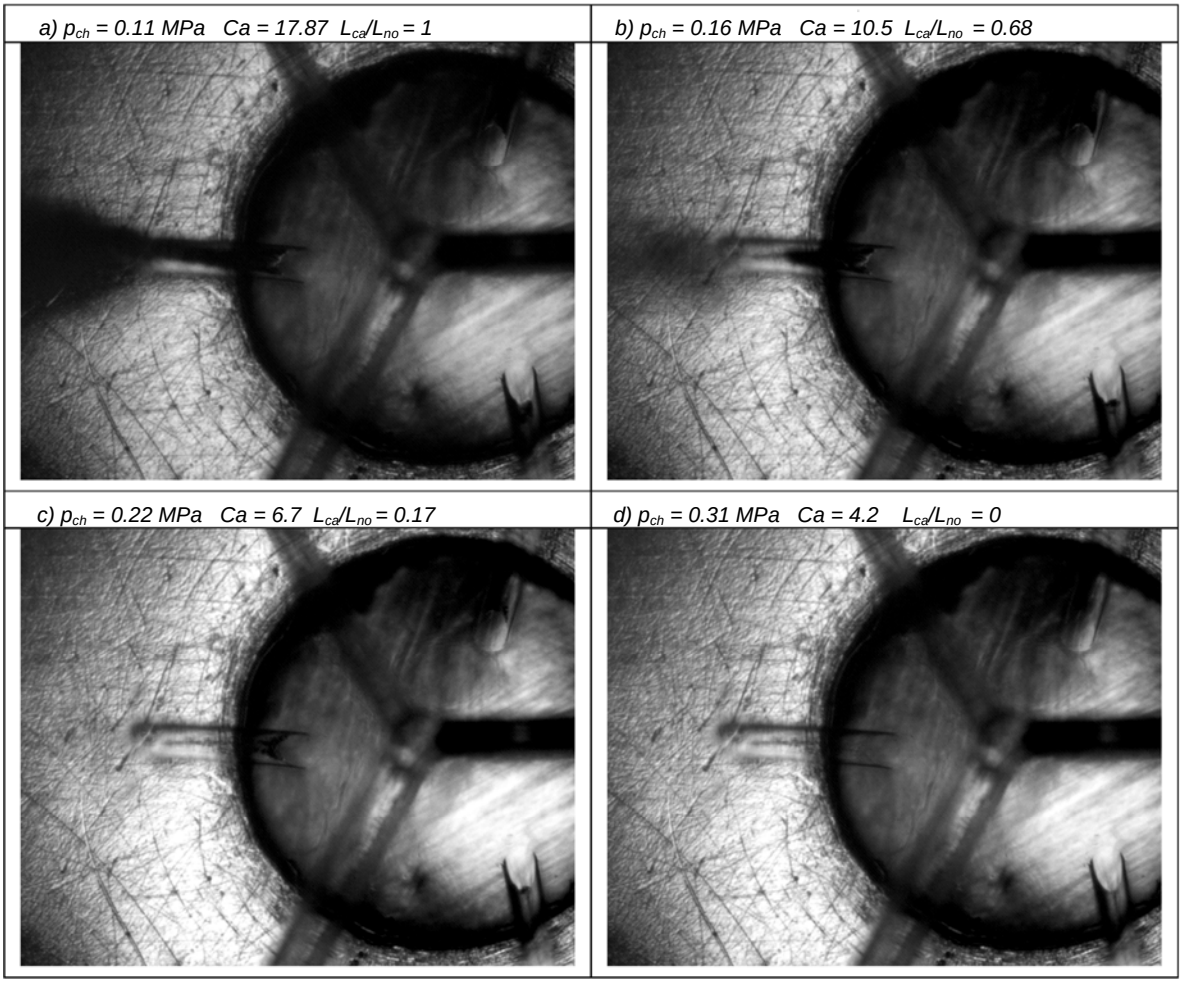

Figure 5. Development of cavitation during a run for a volume fraction of n-pentane φ_2=0.58, an injection pressure p_{inj}=1.42MPa and a relative index of refraction Δn_{ref}=-0,023, the cavitation length shown is for the left orifice.

This work is licensed under a Creative Commons 4.0 International License (CC BY-NC-ND 4.0).

In the following the length of the cavitation voids normalized with the orifice length L_{ca}/L_{no} will be discussed. In the plots each point corresponds to one image and the orifice on the left of the images in figure 5. Firstly, we look at the dependence on the injection pressure shown in Figure 6.

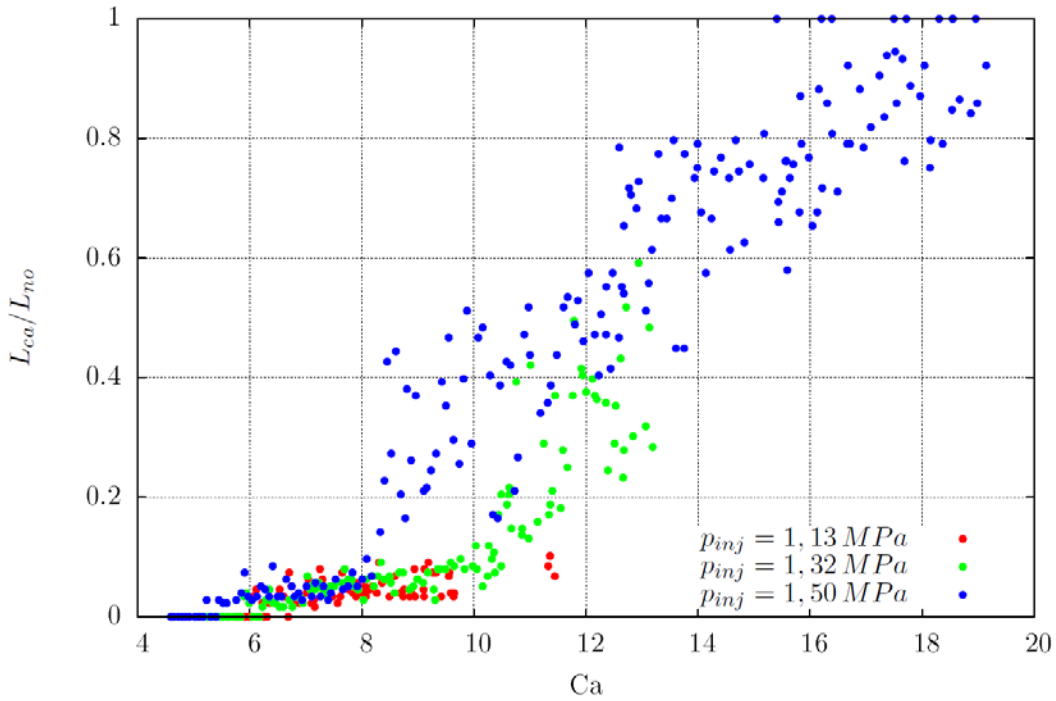

Figure 6. Normalized cavitation length vs. cavitation number for different injection pressures for a mixture with a volume fraction of n-pentane φ_2=*0.45*.

When comparing these results with those for pure liquids [4] the transition of the length of the cavitation voids from a localized area near the inlet of the orifice to supercavitating conditions occurs over a larger span of cavitation numbers. The results for pure n-pentane would range from 3 to 10 independent of the inlet radius. Here it is almost doubled.

It is therefore interesting to look at the dependence of cavitation length for the same injection conditions but for a variation of composition shown in Figure 7. The behaviour of the mixture with the highest n-pentane content comes close to what had been found in [4] for pure n-pentane. With decreasing n-pentane content however the extent of cavitation decreases rapidly. Please bear in mind that the dependence on vapour pressure of the cavitation number has been taken into account by using the vapour pressure of the corresponding mixture. Obviously something is happening here which can not be accounted for by equilibrium thermodynamics. The resulting hypothesis is that a concentration gradient of n-pentane appears in the liquid at the interface to the void because n-pentane evaporates at the interface, the aromatic component has a much lower vapour pressure and fugacity. Therefore the concentration of n-pentane is reduced and diffusion is now limiting since is a relatively slow process. One could argue that the length scales are small. However, the transit time of the liquid through the nozzle is very short also, a few microseconds, and even shorter near the inlet. This could explain why with reduced n-pentane volume fraction in the liquid the voids do not grow to the same extent.

This work is licensed under a Creative Commons 4.0 International License (CC BY-NC-ND 4.0).

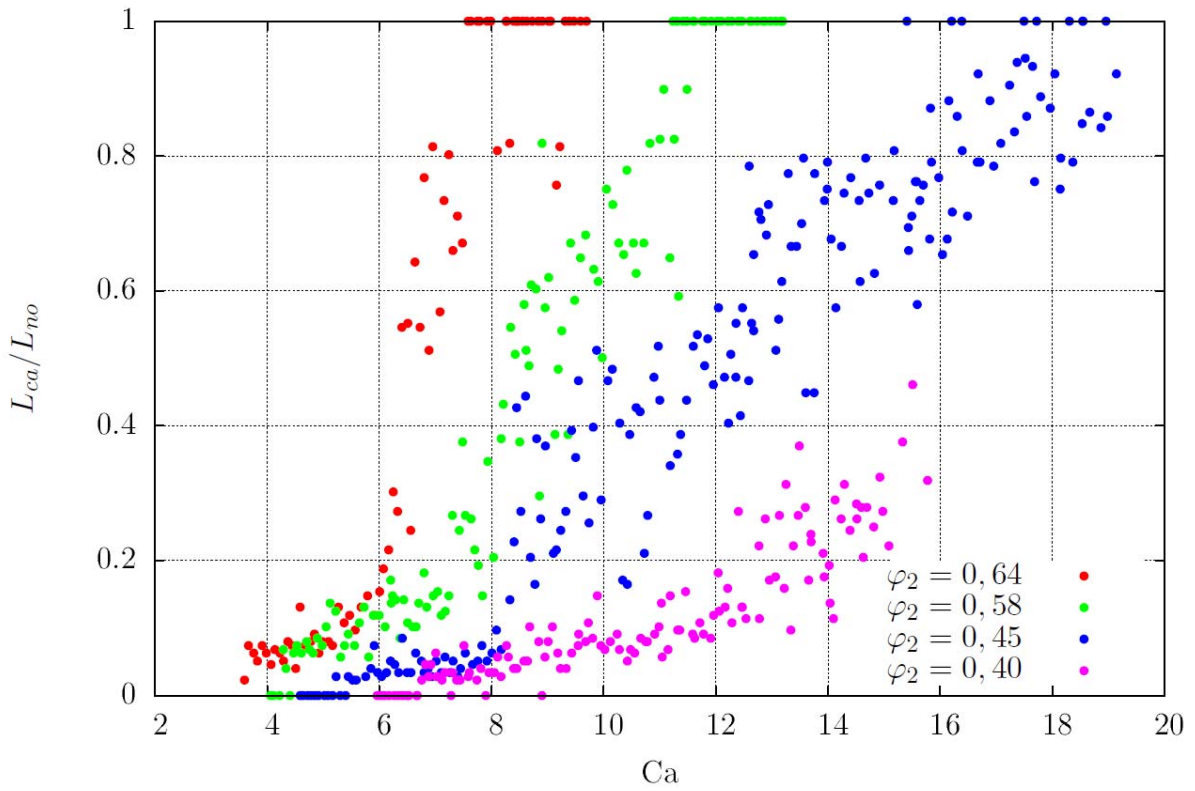

Figure 7. Normalized cavitation length vs. cavitation number for different for various mixtures (volume fraction of n-pentane φ_2) at an injection pressure of about 1.5MPa.

Conclusions

The main conclusion of this paper is that nozzle cavitation depends strongly on the concentration of the components with higher vapour pressure of a mixture. A thermodynamic equilibrium of the concentration of each component at the interface between the phases is not reached within the nozzle.

Acknowledgements

The authors would like to thank Ricard Miranda. He conceived the idea to build a multi-hole nozzle in the way shown here and to Antonio Ortega Planes for his endurance, patience and precision in cutting and polishing the rhombi for the nozzle.

Nomenclature

Ca	cavitation number
L_{ca}	length of cavitation zone in the orifice
L_{no}	orifice length
n	refractive index [-]
n_{fl}	refractive index of fluid mixture [-]
n_{gl}	refractive index of glass of the nozzle [-]
Δn_{rel}	$= (n_{fl}-n_{gl})/n_{gl,}$ relative difference in refractive index between fluid and glass [-]
p_{inj}	injection pressure [Pa]
p_{ch}	chamber or back pressure [Pa]
p_{vm}	vapour pressure from molecular simulations[Pa]
p_{vi}	ideal mixture vapour pressure [Pa]

This work is licensed under a Creative Commons 4.0 International License (CC BY-NC-ND 4.0).

References

[1] Moon, S., Komada, K., Li, Z. , Wang, J., Kimijima, T., Arima, T., Maeda, Y., 2015, Proc. ICLASS 2015, 13th Triennial International Conference on Liquid Atomization and Spray Systems
[2] Mirshahi, M., Nouri, J., Yan, Y., Gavaises, M., Link between in-nozzle cavitation and jet spray in a gasoline multi-hole injector, 2013, Proc. 25th European Conference on Liquid Atomization and Spray Systems
[3 Lichtarowicz, A., 1972, Nature Physical Science Vol. 239
[4] Rewse-Davies, Z., Nouri, J., Gavaises, M. and Arcoumanis, C., Proc. 25th European Conference on Liquid Atomization and Spray Systems, 2013
[5] Marcer, R., Le Cottier, P., Chaves, H., Argueyrolles, B., Habchi, C., Barbeau, B., 2000, SAE Paper 2000-01-2932
[6] Falgout, Z., Linne, M., 2015, Journal of Physics: Conference Series 656 012082
[7] Miranda, R., Chaves, H., Martin, U. and Obermeier, F., 2003, Proc. 9th International Conference on Liquid Atomization and Spray Systems
[8] Payri, R., Salvador, F.J., Gimeno, J., Venegas, O., 2013, Experimental Thermal and Fluid Science 44, pp. 235–244
[9] Payri, R., Gimeno, J., Marti-Aldaravi, P.& Vaquerizo, D., 2015, Atomization and Sprays, 26(9), pp. 889-919
[10] Bode, M., Falkenstein, T., Davidovic, M., Pitsch, H. et al., 2017, *SAE Int. J. Fuels Lubr.* 10(2), doi:10.4271/2017-01-0848.
[11] Falgout, Z. and Linne M., 2016, Review of Scientific Instruments 87, 085108.
[12] Serras-Pereira, J., van Romunde, Z., Aleiferis, P.G., Richardson, D., Wallace, S., Cracknell, R.F., 2010, Fuel 89, pp. 2592–2607.
[13] Miranda, R., Chaves, H., Martin, U. and Obermeier, F., July 13.-17. 2003, 9th International Conference on Liquid Atomization and Spray Systems.
[14] Chaves, H., Bauz, F., Martinez Lopez, E., Sep. 4.-7. 2016, 27th Annual Conference on Liquid Atomization and Spray Systems.
[15] Bergwerk, W., 1959, Proceedings of the Institution of Mechanical Engineers, 173(1), pp. 655⊥ 660.

This work is licensed under a Creative Commons 4.0 International License (CC BY-NC-ND 4.0).

EDITORIAL UNIVERSITAT POLITÈCNICA DE VALÈNCIA